Entrapment of Organic Molecules within Metals. 2. Polymers in Silver

ARTICLE *in* CHEMISTRY OF MATERIALS · JULY 2004

Impact Factor: 8.35 · DOI: 10.1021/cm049824w

Entrapment of Organic Molecules within Metals. 2. Polymers in Silver

Hanna Behar-Levy,† Gennady E. Shter,‡ Gideon S. Grader,‡ and David Avnir*,†

Institute of Chemistry, The Hebrew University of Jerusalem, Jerusalem 91904, Israel and Faculty of Chemical Engineering, Technion, Haifa 32000, Israel

Received February 3, 2004. Revised Manuscript Received May 5, 2004

We describe a new type of composite material: polymers entrapped within a metal. Polystyrene-sulfonic acid and poly(vinyl alcohol) were entrapped within silver. Detailed procedures for the entrapment are provided, and it is shown that this entrapment is a distinctly different process from polymer adsorption on the metal surface. Characterization of these new composites includes XRD measurements, SEM with EDAX, surface area, porosity, and density measurements, and full oxidative degradation analysis by thermogravimetry (TGA/DTA/DTG) coupled to mass spectrometry. A pronounced effect of the metal caging on the thermal degradation of the two entrapped polymers was observed. On the basis of all experimental observations a proposition is made as to the molecular level picture of the entrapment.

1. Introduction

In a recent publication[1] we described a new family of materials, namely organically doped bulk metals. Surprising as this may sound, although organically doped polymers and inorganic materials (e.g., porous sol−gel matrixes[2,3] and inorganic crystals[4]) have been known for decades, the doping of metals seems to have been unexplored.[5] Judging from the many useful properties that have been induced into the organic and inorganic materials by the incorporation of suitable dopant molecules,[2,3,6] and judging from the observations of interesting and useful effects induced by the matrix on dopant properties,[7] one can envisage the potential of similar fruitful applications by the merging of the properties of metals with those of organic molecules. Indeed, while only ∼90 metals are known, there are more than 20 million reported organic molecules, and hence the library of properties which in principle can be induced in metals by the organic dopant, and in the dopant molecules by the metal environment, is enormous.

Whereas our first report[1] dealt with the entrapment of small molecules in a metal, here we focus on the entrapment of polymers. The motivation has been the highly successful merging of organic and inorganic polymers—a huge field by itself—which has led to many new materials, and suffices it to mention as a typical sub-field the organic-polymer modified sol−gel materials.[6,8] Of course, metals and organic polymers have appeared in the same context in various applications, such as in colloidal metals dispersed in polymeric thin films,[9] polymer coatings of metals,[10] surface metallization of polymer surfaces,[11] polymeric particles doped with metals,[12] and more, but not, to the best of our knowledge, in the context of direct doping during synthesis of the metal. Here we describe how to do it with polymers.

Specifically, we demonstrate the feasibility of obtaining such materials by the doping of silver with poly(-4-styrene sulfonic acid) (PSSA) and with poly(vinyl alcohol) (PVA).

* To whom correspondence should be addressed. E-mail: david@chem.ch.huji.ac.il.

† The Hebrew University of Jerusalem.

‡ Technion.

(1) Behar-Levy, H.; Avnir, D. *Chem. Mater.* **2002**, *14*, 1736−1741.

(2) Some recent examples: Zayat, M.; Pardo, R.; Levy, D. *J. Mater. Chem.* **2003**, *13* (12), 2899−2903. Ciriminna, R.; Campestrini, S.; Pagliaro, M. *Adv. Synth. Catal.* **2003**, *345* (11), 1261−1267. Marx, S.; Zaltsman, A. *Int. J. Environ. Anal. Chem.* **2003**, *83* (7−8), 671−680. Lapidot, N.; Gans, O.; Biagini, F.; Sosonkin, L.; Rottman, C. *J. Sol-Gel Sci. Technol.* **2003**, *26* (1−3), 67−72.

(3) Some recent examples from our laboratory: Fireman-Shoresh, S.; Avnir, D.; Marx, S. *Chem. Mater.* **2003**, *15* (19), 3607−3613. Ghattas, A.; Abu-Reziq, R.; Avnir, D.; Blum, J. *Green Chem.* **2003**, *5* (1), 40−43. Gelman, F.; Blum, J.; Avnir, D. *New J. Chem.* **2003**, *27* (2), 205−207.

(4) Benedict, J. R.; Wallace, P. M.; Reid, P. J.; Jang, S. H.; Kahr, B. *Adv. Mater.* **2003**, *15* (13), 1068−1070.

(5) Studies which border our report are the co-sublimation of magnesium and rubrene and, as already mentioned in Part I, the inclusion of impurities during the electrodeposition of metals. Higginson, F. P. *J. Appl. Phys.* **1999**, *85* (8), 4083−4086. Gorbounova, K. M. *Electrochim. Acta* **1959**, *1*, 217−230. Cardenas-Trivino, G. A. J. M.; Klabunde, K. J.; Pantoja, M. O.; Soto, Z. H. *Colloid Polym. Sci.* **1994**, *272*, 310−316. Vermilyea, D. A. *J. Electrochem. Soc.* **1959**, *106*, 66−67.

(6) E.g., Sanchez, C.; Lebeau, B.; Chaput, F.; Boilot, J. P. *Adv. Mater.* **2003**, *15* (23), 1969−1994.

(7) Rottman, C.; Avnir, D. *J. Am. Chem. Soc.* **2001**, *123* (24), 5730−5734. Abu-Reziq, R.; Avnir, D.; Blum, J. *Angew. Chem., Int. Ed.* **2002**, *41* (21), 4132−4134. Abu-Reziq, R.; Blum, J.; Avnir, D. *Chem. Eur. J.* **2004**, *10* (4), 958−962.

(8) E.g., Smarsly, B.; Garnweitner, G.; Assink, R.; Brinker, C. J. *Prog. Org. Coatings* **2003**, *47* (3−4), 393−400. Yu, Y. Y.; Chen, W. C. *Mater. Chem. Phys.* **2003**, *82* (2), 388−395. Sertchook, H.; Avnir, D. *Chem. Mater.* **2003**, *15* (8), 1690−1694.

(9) Andreas Heillmann, H. *Polymer Films with Embedded Metal Nanoparticles*; Springer-Verlag: Berlin, 2002; Vol. 52.

(10) Glebov, E. M.; Yuan, L.; Krishtopa, L. G.; Usov, O. M.; Krasnoperov, L. N. *Ind. Eng. Chem. Res.* **2001**, *40*, 4058−4068.

(11) Warshawsky, A. U. *J. Polym. Sci. Part A: Polym. Chem.* **1989**, *27*, 2963−2994.

(12) Xu, S. Q.; Zhang, J. G.; Kumacheva, E. *Compos. Interface* **2003**, *10* (4−5), 405−421.

10.1021/cm049824w CCC: $27.50
Published on Web 07/09/2004

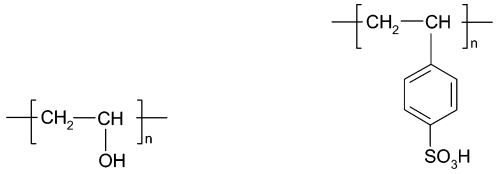

PVA PSSA

Several properties of these new composite materials are reported, and in particular we concentrate on some of their structural aspects, on the mode of entrapment, and on the thermal degradation behavior of the entrapped polymers. It will be shown by simultaneous thermogravimetric and differential thermal analysis (TGA/DTA) with on-line mass spectroscopic analysis (MS) of the exhausted gases that, indeed, the metal−polymer composite affects the thermal oxidative degradation in a novel way.

The doping approach[1] is based on reducing Ag^+ in the presence of a solution of the polymer to be entrapped. The search for suitable reduction conditions included requirements such as efficient removal of the reducing agent and its oxidized products; and a reducing power which is sufficient for affecting the metal cation on one hand, but not the dopant on the other hand. Sodium hypophosphite[13−15] was found suitable from these points of view, and the entrapment is carried out according to

$$\text{polymer} + 2AgNO_3 + NaH_2PO_2 + H_2O \rightarrow \text{polymer@}(2Ag) + NaH_2PO_3 + 2HNO_3 \quad (1)$$

(where the polymer-doped metal is represented by "dopant@metal", e.g., PVA@Ag). NaH_2PO_2 has additional important advantages, namely that the metal-formation procedure can be carried out at room temperature; that no added catalyst is needed; that only water is consumed as an additional reagent (see eq 1); and that the resulting composite retains the classical shine of silver.

2. Experimental Details

Chemicals. Polystyrene sulfonic acid (PSSA) was from Scientific Polymer Products (20% solids in water, MW ∼70 000). Poly(vinyl alcohol) (PVA) (average MW ∼50 000), $AgNO_3$ and $NaH_2PO_2 \cdot \sim 0.2H_2O$ were from Aldrich.

Instrumentation. UV−Vis absorption spectroscopy was carried out with a Hewlett-Packard 8452A diode-array UV−Vis spectrophotometer. XRD measurements were carried out with Philips automated powder diffractometer (with PW1830 generator, PW1710 control unit, PW1820 vertical goniometer, 40 KV, 35 mA, Cu Kα (1.5405 Å)). SEM was carried out with a JEOL JXA SEM 8600 instrument. Energy dispersive analysis of X-rays (EDAX) was carried out with an attachment to the same SEM instrument. Surface area and porosity were determined from nitrogen adsorption/desorption isotherms with a Micromeritics ASAP-2000 physisorption instrument, using the BET and BJH equations, respectively. Density was measured with Quantachrome Multipycnometer 4AC232 instrument using helium as a displacing gas; all samples were pretreated with a flow of helium for 15 min. Elemental microanalyses of carbon and hydrogen were made with Perkin-Elmer 2400-II analyzer. Thermogravimetric and differential thermal analyses (TGA/DTA) were performed simultaneously with a Setaram TGA-92 thermobalance from 25 to 1100 °C at a heating rate of 5 °C/min in flowing dry air (30 cm^3/min). For a more exact analysis of the pyrolysis stages and their temperature ranges, differential thermal gravimetry (DTG) curves were derived from the TGA data using the supplied software. (The DTG curves are not shown, but are available by request from the authors). Mass spectrometry analysis of the TGA exhaust pyrolytic gases was carried out continuously using an on-line quadrupole mass-spectrometer (Thermostar 200, Balzers Co.), coupled and synchronized with the TGA/DTA instrument. The mass spectra were obtained by scanning in the mass range of 2−120 *m*/*z* with a cycle time of 45 s.

Entrapment Procedure of PSSA. A 0.16-g portion of the PSSA solution (0.18 mmol of the repeating monomer unit), 0.2 mL of 1 M NaOH, and 5.0 mL of H_2O were stirred for half an hour to convert the polymer to the sodium salt (which proved to be more suitable for entrapment than the free acid), and the solution was then poured into another stirred solution of 3.03 g (0.018 mol) of $AgNO_3$ in 120 mL of water. Then, 1.5 g (0.017 mol; a 2-fold molar excess, see eq 1) of sodium hypophosphite was added (as solid), and the combined solution was stirred at 150 rpm on a Selecta CELMAG-S stirrer (here and below) at room temperature for 4 days. Precipitation began to be apparent after ∼24 h. The precipitate was filtered, washed with 100 mL of distilled water, and dried for 2 days at 30 °C. The washings contained about 75% of the polymer used in the initial reaction mixture (based on spectroscopic analysis (PSSA in water is characterized by the 261, 268, and 272 nm absorption peaks) and on elemental analysis, which confirmed each other), leaving 25% of it entrapped in the Ag. The amount entrapped can be expressed in several ways: The molar ratio (monomer/Ag) is 1:400, the atomic ratio (C/Ag) is 1:50, and the weight ratio (polymer/Ag) is 1:238 (0.42 w/w%). The PSSA@Ag was stored under nitrogen atmosphere.

Entrapment Procedure of PVA. A 0.008-g aliquot (0.18 mmol of the repeating monomer unit) of PVA was dissolved in 125 mL of water by warming it until total dissolution and then cooling to room temperature. To this solution were added 3.03 g (0.018 mol) of $AgNO_3$ and 1.5 g (0.017 mol) of sodium hypophosphite, and the solution was stirred at room temperature for 4 days. The precipitate was filtered, washed with 100 mL of distilled water to remove the un-entrapped polymer and dried for 2 days at 30 °C. Elemental analysis determined that 75% of the initial PVA was entrapped, resulting in a molar ratio (monomer/Ag) of 1:132, an atomic ratio (C/Ag) of 1:60, and a weight ratio (polymer/Ag) of 1:320 (0.31 w/w%).

Blank Experiments: I. Testing the Stability of the Polymer to the Entrapping Chemicals. Tests were carried out to ensure that neither the reducing agent nor the metal cation affect the polymer. Thus, the silver salt and PSSA were stirred together for 24 h under the above conditions but without the reducing agent; and, likewise, the reducing agent and the polymer were stirred without the silver salt. The PSSA solution was checked spectroscopically in both cases for possible decomposition, but none was found. Similar tests were carried out with PVA, again proving its stability under the entrapping conditions.

II. Extraction Experiments. Further proof of stability was obtained by extracting PSSA from PSSA@Ag, showing that it is the same molecule that has been entrapped. Extractions were carried out with DMSO by stirring 0.1 g of the doped metal with 30 mL of the solvent for 24 h, followed by filtering. Water, a good solvent for the two polymers, was also attempted as an extraction solvent but was found incapable of extracting the polymers; we return to the comparison of the two solvents below.

III. Experiments in Polymer Adsorption on Undoped Silver. To prove that the entrapment is a distinctly different phenomenon from adsorption, the following experiments were carried out. Metallic silver was prepared as described above but without an entrapped polymer. Then, 0.16 g of PSSA solution or 8 mg of PVA and 30 mL of water were stirred for half an hour in the presence of 1.9 g of metallic Ag, and the water was then evaporated to dryness (at 100 °C for 12 h) leaving the polymer adsorbed on the silver.

(13) Krulik, G. A. *J. Chem. Educ.* **1978**, *55*, 361−365.
(14) Ryabukha, A. A. *Inorg. Mater.* **1989**, *25*, 1293−1295.
(15) Vogel, A. J. *A Textbook of Quantitative Analysis*, 3rd ed.; Longmans, Green and Co: London, 1961.

Table 1. X-ray Diffraction Patterns (Angles and Intensities of Doped and Undoped Ag)

plane	literature data[a] Ag		prepared Ag		PSSA@Ag		PVA@Ag	
(*hkl*)	2θ	int	2θ	int	2θ	int	2θ	int
111	38.115	100	38.125	100	38.190	100	38.215	100
200	44.276	40	44.205	38.3	44.390	28.9	44.405	36.1
220	64.423	25	64.415	21.6	64.555	8.8	64.565	11.7

[a] JCPDS, X-ray Powders Diffraction Patterns of Silver, 4-783 (1953).

3. Results and Interpretations

3.1. Entrapment and the Material Properties. We have shown that the two polymers are well entrapped within silver; that the entrapment is distinctly different from adsorption of the polymers on the metal surface (blank experiment III); and that the polymer remains intact upon entrapment (blanks I and II). Thus, elemental analysis revealed an entrapment level of 2.0 % by moles of atom numbers (C atoms per Ag atoms) for PSSA@Ag and 1.7% for PVA@Ag. Both polymers are water-soluble and yet water was not able to extract the polymers. That the polymers are inside the metallic material was evident not only from elemental analysis but also from the successful extraction with DMSO which proved also that the polymer indeed was not affected by the entrapment procedure (see also Blank Experiments). It is not yet clear to us why DMSO can do what water cannot do. Apparently DMSO is capable of disintegrating the nanocrystallites aggregates (described next) by the interaction of the sulfoxide oxygen atoms with the metal surface.

XRD measurements show that the metal is crystalline Ag (Table 1). No peaks of silver salts or silver oxide were seen, and this was confirmed by EDAX analysis of the surface for both doped metals (Figure 1**)** which resulted in 97.86% Ag, some traces of oxygen, and a small amount carbon (partially from the entrapped polymer). On the basis of Scherrer's equation[22] the calculated size of the particles is about 10 nm (Table 2). The elementary particles aggregate (see Figure 2) to form larger crystallites (layered, in the case of PSSA@Ag), several hundreds of nm in size, which then aggregate further to form the macroporous structures, several microns in size, as shown in Figure 2 and in the figure in the Table of Contents. Microporosity and mesoporosity were searched by performing N_2-adsorption−desorption experiments. Representative adsorption−desorption isotherms are shown in Figure 3 for PSSA@Ag and PVA@Ag, and it can be seen that they are indicative of

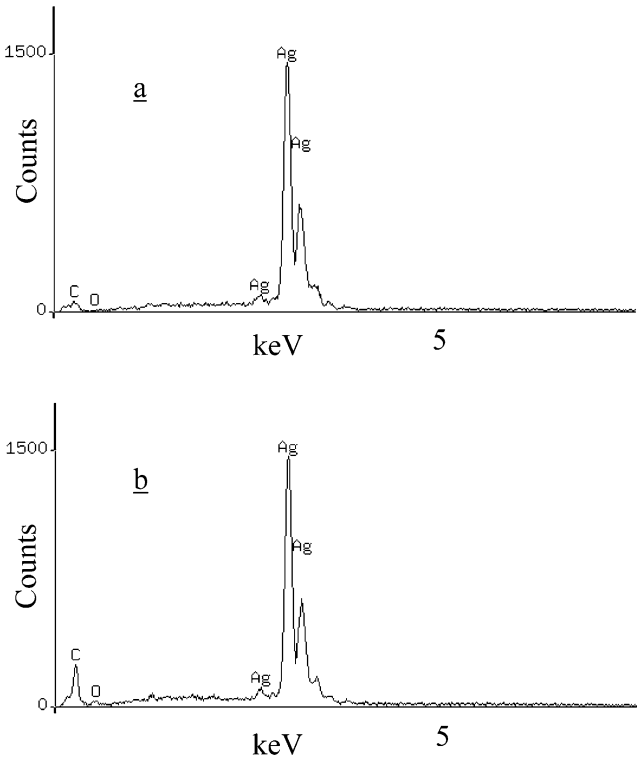

Figure 1. EDAX spectra of (a) silver doped with polystyrenesulfonic acid (PSSA@Ag) and (b) silver doped with poly(vinyl alcohol) (PVA@Ag).

Table 2. Particle Size[a] and Densities

	particle size (nm)	density[b] (g/mL)
silver[c]		10.5
self-made Ag powder	20.2	3.6
PSSA@Ag	9.9	2.6
PVA@Ag	10.7	3.7

[a] The sizes of the particles were calculated from the XRD patterns using Scherrer's equation (ref 22). [b] Measured with a pycnometer. [c] Reference 23.

a mesoporous material. From these isotherms, the nominal BJH pore size, the N_2−BET surface area (an excellent compliance with that equation was obtained; not shown), and *C*-constants were calculated and are collected in Table 3. These data and the apparent densities (which are significantly lower than the density of an Ag crystal; Table 2) indicate an aggregated microcrystalline system which has interstitial porosity, and which hosts the entrapped polymer within this porosity. It should be noted that PSSA affects the properties of the undoped Ag only moderately, but the effect of PVA is significant. The lower surface area, porosity, and *C*-constant of PVA@Ag compared to PSSA@Ag show that whereas PVA tends to fill up the interstitial pores, PSSA is better adsorbed at the interfaces of these pores.

3.2. Thermal Oxidative Degradation of Polymers Entrapped in Silver. The thermal degradation of free PVA[16] and PSSA[17] has been studied intensively where the various decomposition and transformation stages have been elucidated followed by proposed mechanisms of decomposition. Most of these investigations were carried out in an inert atmosphere (nitrogen or argon) with detailed analysis of volatile products which included water, acetaldehyde, acetone, ethanol, benzene, styrene, unsaturated compounds, carbon monoxide and

(16) Holland, B. J. H. *Polymer* **2001**, *42*, 6775−6783.
(17) Jiang, D. D.; McKinney, M. A.; Wilkie, C. A. *Polym. Degrad. Stab.* **1999**, *63*, 423−434.
(18) Li, W. S.; Stampfl, C.; Scheffler, M. *Phys. Rev. Lett*, **2003**, *90*, 256102.
(19) Leventis, N.; Sotiriou-Leventis, C.; Chen, M.; Jain, A. *J. Electrochem. Soc.* **1997**, *144*, L305−308.
(20) Tao, Y. T. *J. Am. Chem. Soc.* **1993**, *115*, 4350−4358.
(21) Tao, Y. T. H.; Chen, L. J. *Langmuir* **2002**, *18*, 8400−8406.
(22) Cullity, B. D. *Elements of X-ray Diffraction*, 2nd ed.; Addison-Wesley, Reading, MA, 1978.
(23) Lide, D. R., Weast, R. C., Selby, S. M., Eds. *CRC Handbook of Chemistry and Physics*; 81st ed.; CRC Press: Boca Raton, FL, 2001.

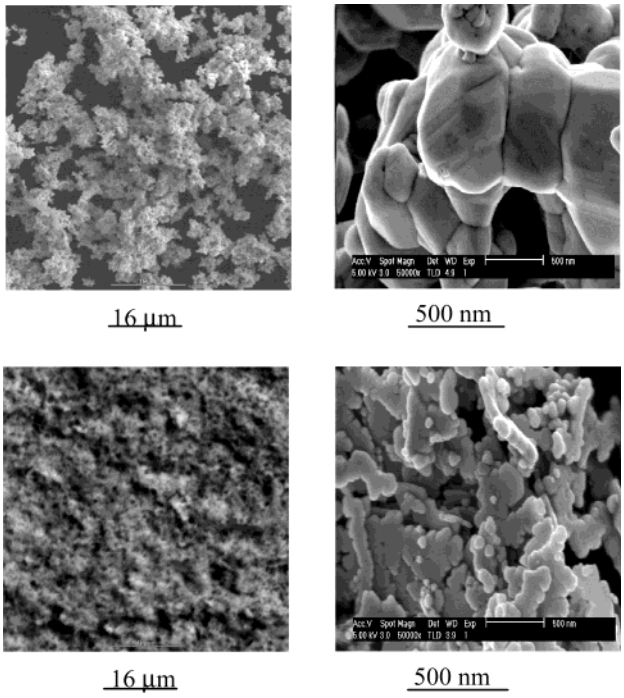

Figure 2. Typical low- and high-resolution SEM pictures of PSSA@Ag (top) and PVA@Ag (bottom).

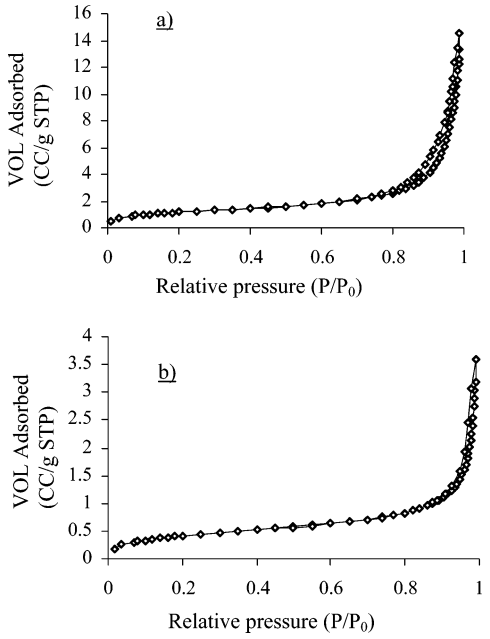

Figure 3. Nitrogen adsorption/desorption isotherms on (a) PSSA@Ag and (b) PVA@Ag.

Table 3. Surface Area and Porosity Values

	surface area (m^2/g)	pore volume (mL/g)	pore size[a] (nm)	BET constant
self-made Ag	5.7	0.02	15	78
PSSA@Ag	4.3	0.02	16	83
PVA@Ag	1.5	0.005	14	59

[a] Nominal BJH values.

dioxide, sulfur dioxide, and more.[16,17] Under oxidative conditions (air) the composition of gases is, of course, greatly shifted to various oxides. As we shall see below, the thermal oxidative degradation behavior of the two polymers while entrapped within silver is affected in a major and, to the best of our knowledge, yet unreported way.

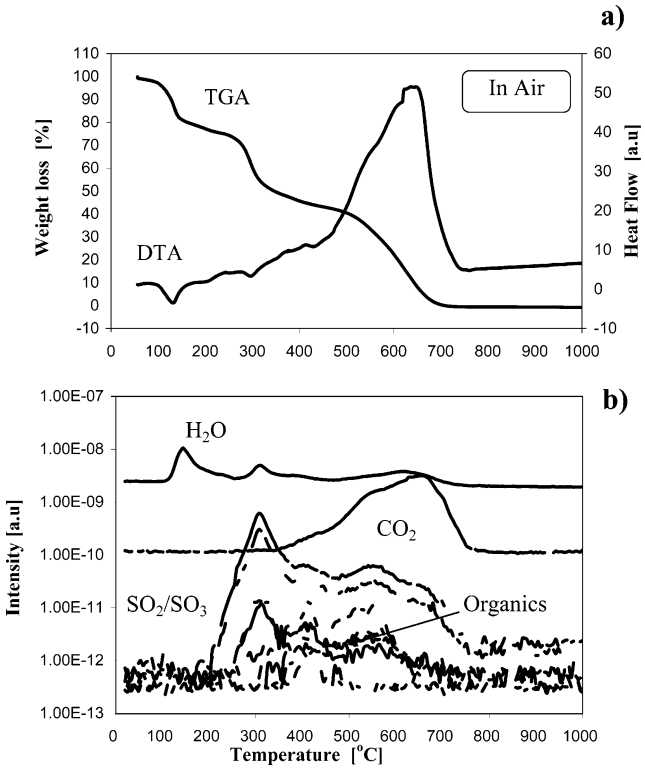

Figure 4. Thermal oxidative degradation of free PSSA: (a) thermal gravimetric analysis (TGA) and differential thermal analysis (DTA), coupled to (b) mass spectrometry.

Thermal Oxidative Degradation (TOD) of PSSA@Ag. To appreciate the major change in the thermal behavior of the metal-entrapped PSSA compared with the free PSSA, we first analyze the TOD behavior of the latter (Figure 4a). Three well-defined weight-loss steps can be seen at the ranges of room-temperature (RT)−200, 200−350, and 350−690 °C. Mass spectrometric analysis of the volatiles (Figure 4b; note the logarithmic scale (here and in the other mass spectra figures below)) helps in identifying the nature of these steps. (i) From RT up to 200 °C the weight loss is mainly due to the release of physisorbed water as seen in its peak slightly above 100 °C. (Note here and below that the baseline for water—and also for CO_2 mentioned below—is high due to traces in the gas carrier and therefore the relevant information here is not the absolute intensity, but the appearance of the peak). (ii) At the 200−350 °C range decomposition of PSSA occurs with significant weight decrease (∼30%) due to further loss of water and to the evolution of SO_2 and SO_3 (as seen by the masses 64, 48, and 24). Indeed, the process of cleavage of the C−S bond is known in the literature to be the first process of degradation.[17] We also show the emissions of many organic fragments (such as styrene (masses of 105, 78, and 50), benzene (78, 52, and 39), and toluene (90, 50, and 39)), although they are minor—orders of magnitude smaller than the main volatiles (even after subtraction of their baselines)—because later on we shall see a quite different behavior for PSSA@Ag. (iii) At 350−750 °C much of the weight loss (∼50%) is due to the oxidation of the organic fragments to CO_2; indeed, a strong exothermic peak characterizes this combustion (Figure 4a).

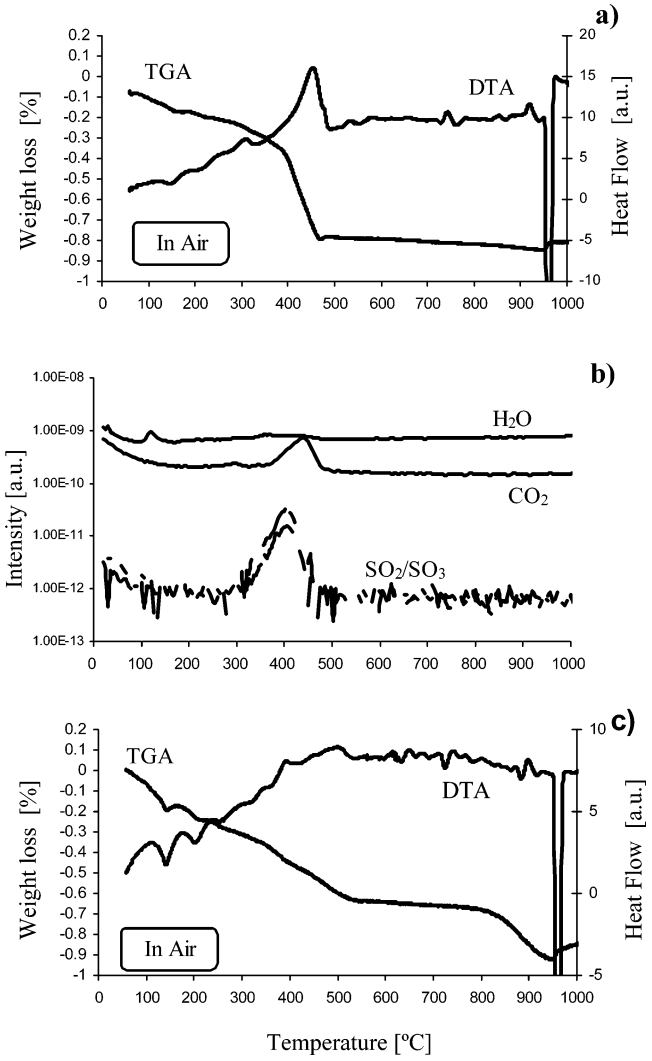

Figure 5. (a) TGA/DTA analysis of PSSA@Ag, coupled to (b) its mass spectrometry, and (c) TGA/DTA analysis of PSSA adsorbed on Ag.

The immediate impression from the TOD curves of PSSA@Ag (Figure 5a) is their simplicity compared to those of the nonentrapped PSSA (Figure 4a). There is one pronounced feature, peaked at ~460 °C of the DTA curve along with a sharp weight loss within a narrow temperature range, which points, first, to *a very efficient oxidative degradation process*, catalyzed by the metal (Ag is a well-known oxidation catalyst[18]); and second, to the homogeneity of the composite material. Two aspects show the catalytic effect. First, the decomposition products are mainly the end oxides SO_2, SO_3, and CO_2 (Figure 5b; very few non-oxidized fragments are observed). Second, the high-temperature region III in Figure 4a practically disappeared—the oxidation is almost completed at 480 °C, almost ~220 °C *lower* than free PSSA. Thus, the CO_2 peak in the MS spectrum—associated with the oxidative process—moves from range of 440−720 °C (Figure 4b) to 380−480 °C in the entrapped state (Figure 5b). Yet on the other hand, the temperature for the beginning of emission of SO_2, SO_3 has moved to higher values for the entrapped polymer (from about 200 °C, Figure 4b, to about 300 °C, Figure 5b). What one sees here is that side-by-side with the *catalyzed decomposition*, there is also an *increase in thermal stability* by a stabilization-through-adsorption mechanism of the polymer, which interacts with the Ag surface through the $-SO_3$ groups (c.f., the affinity of *n*-alkyl sulfonate to gold surfaces which was reported by Levetis et al;[19] similarly, the interaction of carboxylates with metal surfaces is also known[20,21]). In fact, this good dispersion of the polymer contributes to its efficient metal-catalyzed oxidative decomposition. Thus, the combination of these two effects causes an overall significant lowering of the temperature range of decomposition from a range of about 350 °C (Figure 4a) to a range of about 100 °C (Figure 5a).

Another feature worth mentioning in Figure 5a is the sharp endothermic peak at 954 °C which is associated with the melting of Ag (seen also for undoped silver powder prepared by the same procedure). The noticeable (and reproducible) increase of weight during melting, seen in the TGA curve, reflects oxygen chemisorption followed by partial metal oxidation. Interestingly, there is another small but significant weight increase after the catalytic decomposition ends at 480 °C (Figure 5a), which we attribute also to active oxygen chemisorption on Ag after the organic matter was removed. (This weight increase is indeed not observed for pure Ag). The fact that this peak appears only after the removal of the polymer indicates again the strong interaction of the SO_3 atoms with—in fact, activation of—the Ag surface.

Finally, an important blank test which shows that the *entrapment is a different process compared to adsorption* was carried out. In this blank test, the polymer was adsorbed/loaded on the surface of the silver powder, as described in the Experimental Details. It can be clearly seen (Figure 5c) that the TOD behavior of this sample bears absolutely no resemblance to the TOD behavior of PSSA@Ag (Figure 5a) from the points of view of both energy changes (DTA) and weight loss (TGA). The process is quite continuous with no distinct main exothermic effect of oxidative decomposition, Apparently, this continuity is a reflection of diverse interactive populations of the polymer so that some molecular portions are in direct contact with the Ag surface while others are away from it.

Thermal Oxidative Degradation of PVA@Ag. The catalytic effect of Ag on a TOD of a dopant, observed for entrapped PSSA, is confirmed by the TOD behavior of PVA@Ag. First, whereas the main decomposition event of free PVA is around 500 °C (Figure 6a) the entrapped polymer ends its decomposition slightly above 400 °C (Figure 7a; note again the increase in the weight of the silver upon completion of the degradation, as was observed for the entrapped PSSA (Figure 5a). In fact, here this surface oxidation is even more pronounced, apparently because of the rich oxygen content of PVA. Second, the temperature range of the process becomes narrower: from a range of ~310 °C for PVA to ~ 230 °C for PVA@Ag (Figure 7a). And third, the residual non-oxidized and partially oxidized fragments which are clearly seen for PVA (Figure 6b) practically disappear for the entrapped polymer (Figure 7b). Comparative analysis of the major volatiles (Figures 6b and 7b) again shows the effect of fuller oxidation in the entrapped case: the major volatiles are CO_2 and water. Yet PVA@Ag and PSSA@Ag differ in an interesting feature: whereas for PSSA@Ag we have seen that a complex TOD behavior of free PSSA is converted to a

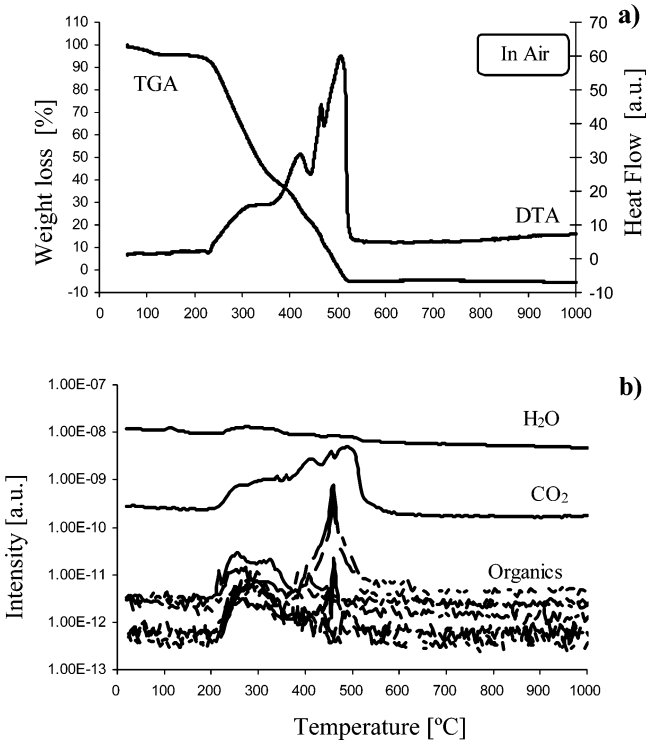

Figure 6. (a) TGA/DTA analysis of free PVA, coupled to (b) its mass spectrometry.

very simple process, in the entrapped polymer for PVA we see conversion of distinct stages (seen clearly in the DTA trace (Figure 6a); see Figure 6b for mass assignment)) into a continuous process, namely a more complex one. This, we believe, reflects a different entrapment mechanism for the two polymers. Whereas PSSA molecules interact tightly with the Ag surface and are in full contact with it (as explained above, through the C−SO_3H moieties), the PVA molecules are more entangled by intra- and intermolecular hydrogen bonds of the CH−OH groups with less pronounced exposure to the Ag surface. Indeed, the TOD of adsorbed PVA (Figure 7c) is even more smeared than the TOD of PVA@Ag, and, in accordance with this proposition, also more smeared than the TOD of adsorbed PSSA (Figure 5a).

4. Conclusions

In this report we described how to prepare a new type of composite material at the border between polymers and metals. Using a large battery of experimental methods we showed that the entrapment is apparently due to entanglement within aggregated nanocrystallites of the metal; that the entrapment is indeed a unique novel process, very different from adsorption; that the entrapment retains the polymers intact; that PSSA and PVA are entrapped differently on a molecular level,

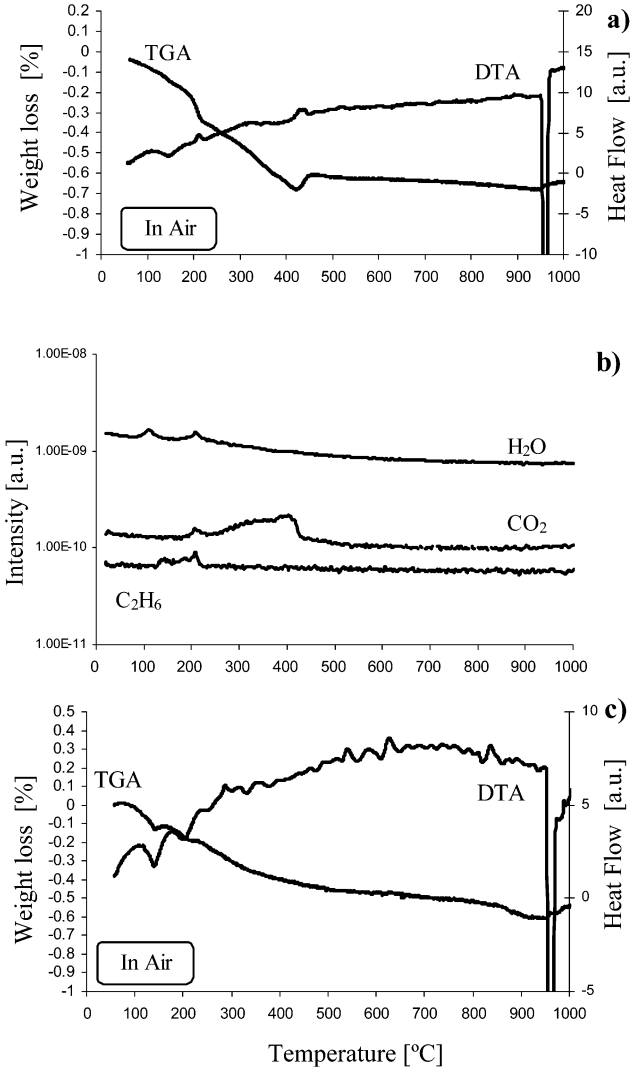

Figure 7. (a) TGA/DTA analysis of PVA@Ag, coupled to (b) its mass spectrometry, and (c) TGA/DTA analysis of PVA adsorbed on Ag.

stabilizing the former; that the thermal oxidative degradation is significantly catalyzed by the metal; and that the composite is quite homogeneous in nature.

We have thus extended the metal entrapment of organics from small molecules[1] to polymers. Other types of metal entrapments, as well as useful applications of these novel composites, will be reported separately.

Acknowledgment. This study was supported by a special grant for Conceptually Novel Research from the Hebrew University, and by a joint grant from the Committee for Planning and Budgeting of the Council for Higher Education and by the Center for Absorption in Science (Israel) under the Kamea program.

CM049824W